Photoexcited States

DOI: 10.1002/ange.200600898

First Evidence for a Uniquely Spin-Polarized Quartet Photoexcited State of a π-Conjugated Spin System Generated via the Ion-Pair State**

Yoshio Teki, Hirotaka Tamekuni, Jun Takeuchi, and Yozo Miura*

Switching of physical properties by external stimuli has attracted much attention in investigations on functional materials.[1] Manipulation of the magnetic properties of organic molecules in the spin ground state has been intensively studied by using electron-hole doping[2] and photochromic molecules.[3] Recently, photoswitching between diamagnetic and paramagnetic phases was realized in a 1,3,5-trithia-2,4,6-triazapentalenyl (TTTA) organic crystal.[4] Studying spin alignment in photoexcited states will give key knowledge for the photocontrol of magnetic properties. We have reported photoexcited quartet ($S = 3/2$) and quintet ($S = 2$) high-spin states of π-conjugated organic compounds[5–7] constructed from aromatic hydrocarbons and pendant stable radicals. π-Conjugated spin systems lead to robust spin alignment compared with other triplet/radical-pair systems (σ-bonded systems[8] and coordination complexes[9]). In the quintet state,[5,6] photoinduced spin alignment between two pendant radicals was achieved through the triplet excited state of a diphenylanthracene moiety, and exchange coupling between the two radicals changes from antiferromagnetic to ferromagnetic on photoexcitation. This example is the first of spin manipulation of π radicals in the photoexcited state.

Coupling spin alignment to photoinduced electron transfer (PET) or energy transfer is the next important fundamental research target for the photocontrol of organic magnetism. As a model compound, we designed **1**, in which a 4,4-difluoro-4-bora-3a,4a-diaza-*s*-indacene (bodipy) acceptor moiety (A),[10] is covalently linked through an

[*] Prof. Dr. Y. Teki, H. Tamekuni
Department of Material Science
Graduate School of Science
Osaka City University
3-3-138 Sugimoto, Sumiyoshi-ku, Osaka 558-8585 (Japan)
Fax: (+81) 6-6605-2559
E-mail: teki@sci.osaka-cu.ac.jp
J. Takeuchi, Prof. Dr. Y. Miura
Department of Applied Chemistry
Graduate School of Engineering
Osaka City University
3-3-138 Sugimoto, Sumiyoshi-ku, Osaka 558-8585 (Japan)

[**] This work was supported by a Grant-in-Aid for Scientific Research on the General (No. 16350079) and Priority Area "Application of Molecular Spin" (Area 769, Prop. No. 15087208) from the Ministry of Education, Culture, Sports, Science and Technology (MEXT), Japan.

Supporting information for this article is available on the WWW under http://www.angewandte.org or from the author.

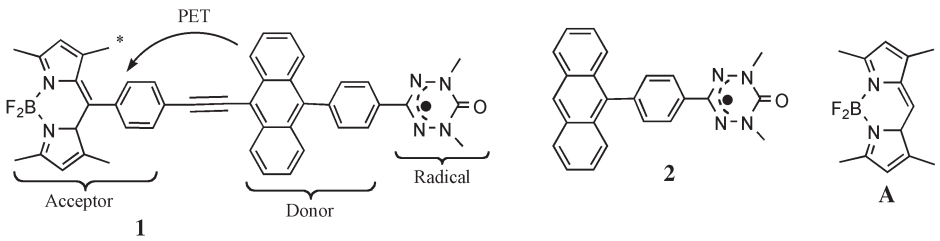

anthracene moiety, as a donor (D) to the verdazyl π radical (R). π-Conjugated system **2** (D–R) has a quartet ($S = 3/2$) photoexcited state. The bodipy moiety is well known as an efficient through-bond energy acceptor for anthracene.[10] Herein, we present the first evidence of a uniquely spin-polarized quartet photoexcited state generated by a novel spin-polarization mechanism via the ion-pair state. Compound **1** was synthesized according to Scheme 1.[11]

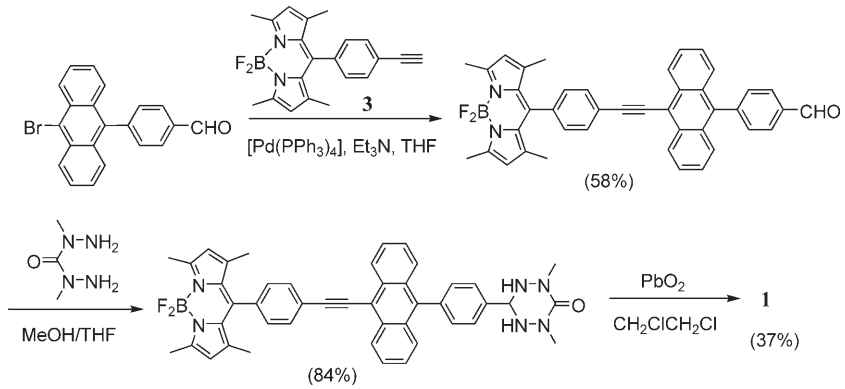

Scheme 1. Synthesis of **1**.

The UV/Vis spectrum of a solution of **1** in toluene showed a sharp band at 505 nm (Figure 1) that arises from the acceptor A. This band overlaps with the weak n→π transition of the verdazyl radical R. The absorption bands characteristic of the anthracene moiety are red-shifted by about 40 nm relative to **2** (320–420 nm bands), indicative of an interaction between D and A. The oxidation potential of phenylanthracene is slightly higher than that of component A.[10] Thus, there is no charge transfer (CT) character in the ground state. However, if one-electron photoexcitation from the highest occupied molecular orbital (HOMO) of A is carried out, the orbital becomes lower in energy because the on-site Coulomb repulsion is removed. Therefore, A* will act as an electron acceptor for D and PET occurs immediately in **1** through π conjugation. In the photoexcited state of **1**, the bodipy component will act as an "electron acceptor" (A*) and the phenylanthracene moiety plays the role of an electron donor (D).

To learn more about the photoexcited state, we measured time-resolved electron spin resonance (TRESR) and pulsed ESR spectra synchronized to pulsed laser excitation. The TRESR spectrum of **1** (Figure 2a) was observed 0.3 μs after laser excitation of the absorption band ($\lambda =$ 505 nm) of component A. Almost the same spectrum was obtained by excitation of the absorption band ($\lambda = 447$ nm) of the anthracene moiety. The emission spectrum characteristic of bodipy (see the Supporting Information) was obtained by excitation of D as well as of component A. These findings show that efficient energy transfer occurs from the anthracene moiety D to A. The spin Hamiltonian parameters of **1** were determined to be $S = 3/2$, $g = 2.0035$, $D = 0.0215\ \mathrm{cm}^{-1}$, and $E = 0.001\ \mathrm{cm}^{-1}$ by spectral simulation (Figure 2b), with the hybrid eigenfield/exact diagnonalization method taking

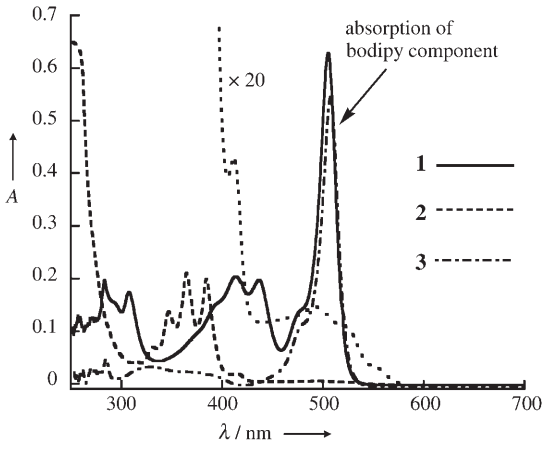

Figure 1. UV/Vis absorption spectra of solutions of **1** and **3** in toluene and **2**[6] in 2-methyltetrahydrofuran. The absorbance of **1** and **3** is not well-reproduced in the range 250–285 nm as a result of overlap with absorptions from the toluene solvent.

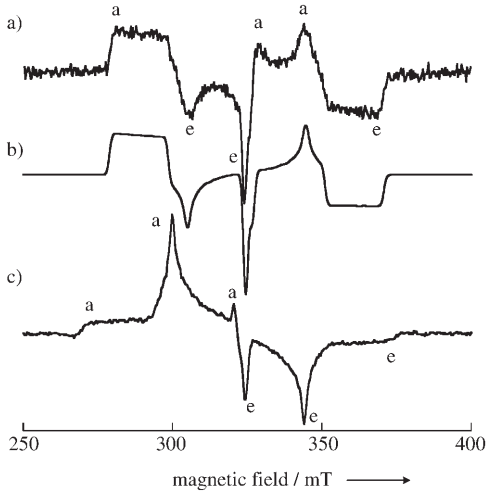

Figure 2. TRESR spectra of **1** and **2** at 30 K in glass matrices; a: absorptions; e: emissions of microwaves. a) Observed spectrum of **1**; b) simulation; c) observed spectrum of **2**.

dynamic electron polarization (DEP) into account.[12] This magnitude of D is about 7% smaller than that of **2**[6] and indicates delocalization of the unpaired electron toward acceptor moiety A. Comparison with the TRESR spectrum of **2** (Figure 2c) clearly shows that the DEP phase pattern of **1** (aeeaae) is different to that of **2** (aaaeee). This unique DEP is generated by attachment of the bodipy functional group.

To confirm the spin state, spin-echo-detected transient nutation (TN) spectroscopy[13] was carried out. Figure 3

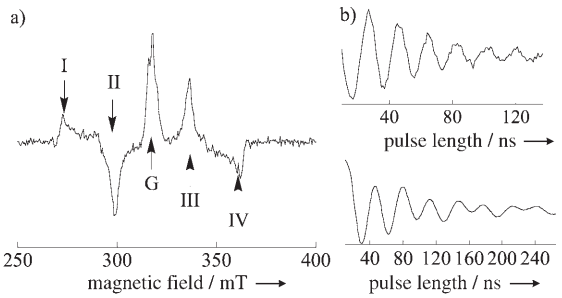

Figure 3. Pulsed ESR spectra of **1**. a) Echo-detected ESR spectrum; b) typical TN behavior (top: quartet signal at 337 mT; bottom: ground-state signal without photoexcitation).

depicts the echo-detected ESR spectrum observed 0.3 μs after pulsed laser excitation and typical TN behavior of the photoexcited and ground states. The strong center signal is a superposition of the $M_s = -1/2 \leftrightarrow +1/2$ transition arising from the ground and photoexcited states. Other signals come from the photoexcited state, as was confirmed by the spectrum without photoexcitation. The spectral pattern of the signals as a result of the photoexcited state is almost the same as that of the TRESR spectrum, in that all signals have similar phase-memory times and spin–lattice relaxation times.[7] Under the condition $\omega_1 \ll \omega_{ZFS}$, the TN frequency ω_{TN} of the $M_s \leftrightarrow (M_s+1)$ transition is given by Equation (1),[13] where $\omega_1 = g\beta B_1/\hbar$,

$$\omega_{TN} = \sqrt{S(S+1) - M_s(M_s+1)}\,\omega_1 \quad (1)$$

$\omega_{ZFS} = D/\hbar$, and B_1 is the microwave-field strength. Therefore, in the quartet state, the expected TN frequencies for $M_s = \pm 1/2 \leftrightarrow \pm 3/2$ and $M_s = -1/2 \leftrightarrow +1/2$ allowed transitions are $\sqrt{3}\omega_1$ and $2\omega_1$, respectively. For the ground state, ω_{TN}^G is equal to ω_1, because **1** has a doublet ground state ($S = 1/2$).

The observed ratios $\omega_{TN}^{EX}/\omega_{TN}^{G}$ for each transition indicated in Figure 3 by arrows are close to $\sqrt{3}$ (Table 1), which is expected for the ratio of the TN frequencies between the quartet and the doublet states. The TN experiments show unambiguously that all signals indicated by arrows are assigned to $M_s = \pm 1/2 \leftrightarrow \pm 3/2$ transitions of the quartet state. The center signal attributed to $M_s = -1/2 \leftrightarrow +1/2$ transitions showed a complicated TN behavior. Fourier transformation gave a power spectrum with multifrequencies,

Table 1: Ratios $\omega_{TN}^{E}/\omega_{TN}^{G}$ of TN frequencies of each transition of **1** (see Figure 3).

I	II	III	IV
1.75	1.66	1.76	1.74

which consist of $2\omega_1$, ω_1, and lower-frequency signals (possible off-resonance transition).

The quartet photoexcited states of triplet/radical pairs reported so far in the solid phase are formed by spin–orbit intersystem crossing (SO-ISC) of the parent triplet state,[8,9] or by enhanced SO-ISC by π conjugation with the pendant radical.[5–7] In such cases, the SO-ISC mechanism generates selective population of the zero-field (ZF) wave functions of the quartet spin states, thus leading to an A/E (aaaeee) or E/A (eeeaaa) pattern. In contrast, for the two-spin system, it is well-known that the radical-pair (RP) mechanism[14] in solution leads to selective population of the high-field (HF) wave functions of the M_s sublevels by singlet–triplet mixing S–T_0 (or S–$T_{\pm1}$). The DEP depends on the pathway that leads to the observed state. Thus, the DEP pattern gives evidence for the dynamic process generating the observed state. Spectral simulation (Figure 2b) was carried out by assuming selective population both for the ZF and HF wave functions (ZF/HF = 0.45:0.55). Judging from the resonance field, the central peak at 325 mT is a superposition of the polarized ground-state signal, which is included in the simulation (see the Supporting Information). Thus, a competition between SO-ISC and other mechanisms occurs in **1**. Similar competitions between SO-ISC and RP mechanisms have been observed only in the reaction centers of photosystems I and II[15] and in their model systems via the ion-pair (IP) state.[16]

We propose a model to understand the unique spin polarization of the quartet photoexcited state of **1**. Immediately after photoexcitation, component A reaches the singlet photoexcited state (S_1). In this state, PET occurs immediately from D to A through the π conjugation in **1**[17] and leads to the charge-separated IP state $A^{\bullet-}$-$D^{\bullet+}$-R, in which $A^{\bullet-}$ is the doublet state and ab initio MO calculations show that the cation of **2** ($D^{\bullet+}$-R) becomes the triplet ground state ($|T\rangle$). In this charge-separated IP state, the electron spins of $A^{\bullet-}$ and $D^{\bullet+}$ are far apart and their exchange coupling is very weak (Figure 4). As a consequence, the wave functions of the doublet and quartet states are mixed as given in Equations (2).

$$\phi_1;\ |T_{+1},\alpha\rangle = |Q_{3/2}\rangle \quad (2a)$$

$$\phi_2;\ |T_{+1},\beta\rangle = \sqrt{\frac{1}{3}}|Q_{1/2}\rangle + \sqrt{\frac{2}{3}}|D_{1/2}\rangle \quad (2b)$$

$$\phi_3;\ |T_0,\alpha\rangle = \sqrt{\frac{2}{3}}|Q_{1/2}\rangle - \sqrt{\frac{1}{3}}|D_{1/2}\rangle \quad (2c)$$

$$\phi_4;\ |T_0,\beta\rangle = \sqrt{\frac{2}{3}}|Q_{-1/2}\rangle + \sqrt{\frac{1}{3}}|D_{-1/2}\rangle \quad (2d)$$

$$\phi_5;\ |T_{-1},\alpha\rangle = \sqrt{\frac{1}{3}}|Q_{-1/2}\rangle - \sqrt{\frac{2}{3}}|D_{-1/2}\rangle \quad (2e)$$

$$\phi_6;\ |T_{-1},\beta\rangle = |Q_{-3/2}\rangle \quad (2f)$$

The sublevels ϕ_2–ϕ_5 will be selectively populated, because the initial state generated by photoexcitation is the doublet excited state. During the charge-recombination process, these weakly coupled wave functions ϕ_2–ϕ_5 change to the strongly

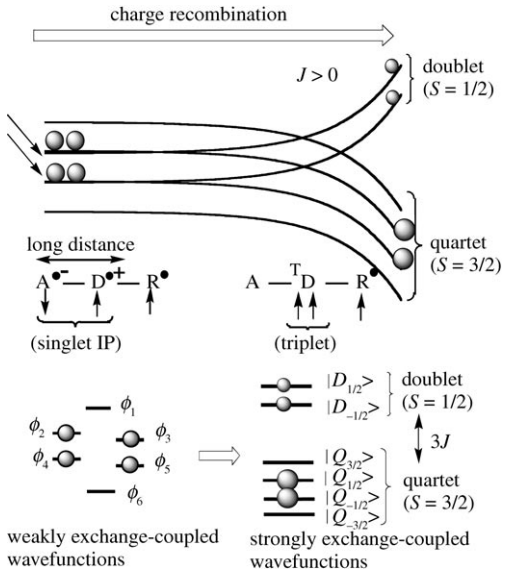

Figure 4. Mechanism of DEP generation in the quartet excited state of **1** through the IP state. *J* is the magnitude of the effective exchange coupling between unpaired electrons. The magnitude of population transfer from the weakly coupled wave functions to those of the pure quartet and doublet states depends on the duration of the charge-recombination process and the Δg value.

exchange-coupled pure doublet ($|D_{\pm1/2}\rangle$) and quartet wave functions ($|Q_{\pm1/2}\rangle$), thus leading to DEP (Figure 4). The ISC and the selective population (DEP) of the high-field wave functions of the quartet state are also expected to depend on D–Q mixing driven by the difference in *g* values Δg and in hyperfine interactions, similar to $S–T_0$ mixing of the triplet/radical pair. In other words, as a result of M_s conservation, population of the charge-separated IP state (left side of Figure 4) can selectively move to the $M_s = \pm 1/2$ spin sublevels $|D_{\pm1/2}\rangle$ and $|Q_{\pm1/2}\rangle$ (right side of Figure 4), which leads to a non-Boltzmann population (DEP). This mechanism via the intramolecular doublet–triplet IP state will occur in the solid, liquid, and gas phases and compete with the enhanced SO-ISC mechanism derived from the pendant radical. Unfortunately, direct detection of the IP state by transient absorption spectroscopy was unsuccessful, because strong emission from the bodipy component masks the absorption band of the anthracene radical cation. However, the unique spin polarization pattern observed by both TRESR and pulsed ESR spectroscopy gives clear evidence of the IP state $A^{\bullet-}$-$D^{\bullet+}$-R as the photoexcited state. This observation is the first of a photoexcited quartet state generated through the IP state of an organic molecule with unpaired spins.

Experimental Section

Optical, TRESR, and pulsed ESR mesurements: UV/Vis spectra were measured on a JASCO V-570 spectrometer at room temperature. A conventional X-band ESR spectrometer (JEOL TE300) was used without field modulation in the TRESR measurements. Signals were amplified by a wide-band preamplifier, transferred to a high-speed digital oscilloscope (LeCroy 9350C), and accumulated for each point. Excitation of **1** was carried out at 505 nm with light from an optical parametric oscillator (OPO) system pumped by a YAG laser (Continuum Surelite II-10 and Surelite OPO). The temperature was controlled by an Oxford ESR 910 cold He gas flow system. All TRESR and pulsed ESR experiments were carried out with toluene as the glass matrix or solvent. Samples were degassed by repeated freeze–pump–thaw cycles. The pulsed ESR measurements were performed on an X-band ESR spectrometer equipped with a pulsed microwave unit (JEOL ES-PX1150) and a high-speed digital oscilloscope (Tektronix TDS5034). The pulsed microwaves were amplified with a 1-kW traveling wave tube amplifier (TWTA). The Hahn $\pi/2$–τ–π pulse sequence was used for spin-echo detection. The microwave pulse was synchronized with the laser excitation by using a delay-pulse generator (Stanford Research DG535). In the echo-detected nutation experiment, the first microwave pulse length was varied.

Materials: The stable radical **1** was synthesized according to the procedures shown in Scheme 1.[11] Compound **3** was prepared according to the literature method.[10] Other reagents were used as purchased. Column chromatography was performed on silica gel (Merk Silica 60) or alumina (Merk Alum. Ox. 60).

Received: March 8, 2006
Published online: June 22, 2006

Keywords: donor–acceptor systems · EPR spectroscopy · ion pairs · photochemistry · radicals

[1] See: *Proceedings of the 9th International Conference on Molecule-based Magnets* (*Polyhedron* **2005**, *24*, 2063–2912).
[2] A. Izuoka, M. Hiraishi, T. Abe, T. Sugawara, K. Sato, T. Takui, *J. Am. Chem. Soc.* **2000**, *122*, 3234.
[3] a) K. Matsuda, M. Irie, *J. Am. Chem. Soc.* **2001**, *123*, 9896; b) K. Takayama, K. Matsuda, M. Irie, *Chem. Eur. J.* **2003**, *9*, 5605.
[4] H. Matsuzaki, W. Fujita, K. Awaga, H. Okamoto, *Phys. Rev. Lett.* **2003**, *91*, 017403.
[5] a) Y. Teki, S. Miyamoto, K. Iimura, M. Nakatsuji, Y. Miura, *J. Am. Chem. Soc.* **2000**, *122*, 984; b) Y. Teki, S. Miyamoto, K. Iimura, M. Nakatsuji, Y. Miura, *J. Am. Chem. Soc.* **2001**, *123*, 294.
[6] Y. Teki, M. Nakatsuji, Y. Miura, *Mol. Phys.* **2002**, *100*, 1385.
[7] Y. Teki, T. Toichi, S. Nakajima, *Chem. Eur. J.* **2006**, *12*, 2329, and references therein.
[8] a) C. Corvaja, M. Maggini, M. Prato, G. Scorrano, M. Venzin, *J. Am. Chem. Soc.* **1995**, *117*, 8857; b) J. Fujiwara, Y. Iwasaki, Y. Ohba, S. Yamauchi, N. Koga, S. Karasawa, M. Fuhs, K. Möbius, S. Weber, *Appl. Magn. Reson.* **2001**, *21*, 483, and references therein.
[9] a) K. Ishii, J. Fujiwara, Y. Ohba, S. Yamauchi, *J. Am. Chem. Soc.* **1996**, *118*, 13079; b) K. Ishii, Y. Hirose, N. Kobayashi, *J. Phys. Chem.* **1999**, *103*, 1986.
[10] C. W. Wan, A. Burghart, J. Chen, F. Bergeström, L. Joansson, M. F. Wolford, T. G. Kim, M. R. Topp, R. M. Hochstrasser, K. Burgess, *Chem. Eur. J.* **2003**, *9*, 4430.
[11] **1**: Elemental analysis (%) calcd for $C_{45}H_{36}BF_2N_6O$: C 74.49, H 5.00, N 11.58; found: C 73.95, H 4.79, N 11.14; HRMS (FAB^+, 3-NBA matrix): *m*/*z* calcd for $[M^+]$: 725.3012; found: 725.3007.
[12] The details of the spectral simulation are similar to those described in reference [5b], with Equation (6) from reference [5b] being modified as follows: $P_{MS} = w1\,P_{M_s}^{\text{zero field}} + w2\,P_{M_s}^{\text{high field}}$, $w1 = 0.45$, and $w2 = 0.55$, as described in the text. $P_{M_s}^{\text{zero field}}$ is the expectation value of the density matrix, which represents the populations of the zero-field spin sublevels and $P_{M_s}^{\text{high field}}$ is that of the high-field spin sublevels ($|S,M_s\rangle$). The doublet ground state was independently simulated using the *g* value determined experimentally and superimposed to the quartet spectrum (see the Supporting Information). More details will be published in a full paper.

[13] a) J. Isoya, H. Kanda, J. R. Norris, J. Tang, M. K. Bowman, *Phys. Rev. B* **1990**, *41*, 3905; b) A. V. Astashkin, A. Schweiger, *Chem. Phys. Lett.* **1990**, *174*, 595.
[14] F. J. Adrian, *J. Chem. Phys.* **1974**, *54*, 3918.
[15] H. Levanon, J. R. Norris, *Chem. Rev.* **1978**, *78*, 185.
[16] a) K. Hasharoni, H. Levanon, S. R. Greenfield, D. J. Gosztola, W. A. Svec, M. R. Wasielewski, *J. Am. Chem. Soc.* **1995**, *117*, 8055; b) K. Hasharoni, H. Levanon, S. R. Greenfield, D. J. Gosztola, W. A. Svec, M. R. Wasielewski, *J. Am. Chem. Soc.* **1996**, *118*, 10228.
[17] The π conjugation leads to the wavelength shift (ca. 40 nm) of the anthracene moiety in the absorption spectrum shown in Figure 1. The magnitude of the interaction between D and A is estimated to be about 2300 cm^{-1} from the shift. Such a large interaction cannot be a through-space interaction. Therefore, it is clear that PET is a through-bond effect in this case.

